

## Strengthening of RC flat slabs against punching shear with GFRP laminates adopting a hybrid technique

Amr M. Ibrahim\* and Mohamed S. Fawzy

Department of Civil Engineering, The British University in Egypt, El-Shorouk, Egypt

Received 11 June 2023  
Revised 3 September 2023  
Accepted 12 September 2023

### Abstract

Punching shear failure at the slab-column connection is one of the foremost concerns associated with reinforced concrete (RC) flat slabs. Many strengthening techniques of existing RC flat slabs against punching shear failure have been developed, one of which is an innovative hybrid strengthening technique that combines two different approaches which are near surface mount (NSM) and embedded through sections (ETS). This paper evaluates the potentialities of utilizing this hybrid strengthening technique using glass fiber reinforced polymer (GFRP). Also, this research intends to numerically investigate the influence of some key parameters on the punching shear strength of the slab. Moreover, the efficiency of the analytical approach for determining the punching shear strength of RC flat slabs using the critical shear crack theory (CSCT) is evaluated for RC slabs strengthened with GFRP laminates adopting the hybrid technique. The finite-element model used in this study is described and the relevant results are discussed.

**Keywords:** Flat slabs, Punching shear strengthening, GFRP laminates, Numerical simulation, CSCT, Abaqus

### 1. Introduction

Flat slabs are one of the most used reinforced concrete (RC) slab systems around the world as a result of their ease of construction, reasonable construction cost, and ability to provide relatively large spans. Flat slabs are in direct connection with columns with no beams in between. Despite the many advantages provided by this system, there is a major concern regarding its design which is the two-way shear failure, also known as punching shear failure. This failure has a brittle nature, and it is associated with very limited warning signs, so it has the potential to cause a progressive collapse of the entire building [1]. Punching shear failure occurs as a result of flexural and shear stress concentration at the proximity area of the columns and it takes the shape of a frustum of a pyramid for square columns and a frustum of a cone for circular columns [2, 3]. Nevertheless, punching shear failure can be a concern not only for the design of RC flat slabs but also for existing RC flat slabs. Several reasons can cause punching shear failure in existing RC structures such as increasing the vertical loads on the slab, not using proper materials as per design, errors in construction, or not complying with the latest code provisions.

Punching shear failure takes place whenever the two-way shear stress acting on the slab exceeds the punching strength of the slab. According to the critical shear crack theory (CSCT) developed by Muttoni [4], the punching strength of flat slabs is governed by two relations: the load-rotation relationship and the failure criterion. The load-rotation relationship relates to the flexural strength of the slab, and it can be obtained analytically or by using numerical simulation [4]. While failure criterion is a semi-empirical relation that relates the punching strength of the slab to the crack width [5, 6]. The punching shear strength, in turn, is the intersection point between these two curves [4]. So, for the punching shear strength of the slab to be improved, one of these two curves, or both, need to be raised. Some strengthening techniques of RC flat slabs against punching shear failure influence either one of the load-rotation curve or the failure criterion, while other techniques influence both curves. CSCT has successfully been applied to predict the punching shear strength of RC flat slabs strengthened with different strengthening techniques as concluded by Lapi et al. [7].

Many techniques for strengthening existing RC flat slabs against punching shear failure have been developed over the past years. The most common of which are enlargement of the support, flexural strengthening, and shear strengthening [7].

Enlargement of the support can be achieved by widening the column section, or by inserting steel or concrete capital at the area of connectivity between the slab and the column [8, 9]. The experimental results obtained by Hassanzadeh and Sundqvist [10] showed that the inserted capital worked as a column head that was poured with the column from the beginning. This technique affects both the load-rotation curve and the failure criterion curve [7].

Flexural strengthening can be achieved using one of two approaches: Externally bonded reinforcement (EBR) approach or Near surface mount (NSM) approach [10-12]. EBR approach is performed by bonding fiber reinforced polymer (FRP) or steel laminates or sheets on the tension surface of the slab, while NSM approach is performed by introducing FRP or steel laminates into pre-executed grooves in the tension side of the slab. Whilst both approaches improve the flexural strength of the slab, NSM approach is more

\*Corresponding author.

Email address: amr.ibrahim@bue.edu.eg

doi: 10.14456/easr.2023.51

effective because a better bond strength between the concrete and the laminates is provided reducing the potential occurrence of premature failures such as laminate slippage, as discussed in the publications [12-16]. This technique only affects the load rotation curve with almost no influence on the failure criterion curve [7].

Regarding shear strengthening as it was addressed by Meisami et al. [17], it can be achieved by using Embedded through sections (ETS) approach which is based on inserting steel or FRP dowels or bars into vertical or inclined holes drilled into the slab depth. This technique only affects the failure criterion without affecting the load-rotation curve [7].

While shear strengthening and flexural strengthening techniques are typically applied separately to either solely improve the flexural or shear strength of the slab; consequently, raising either the load-rotation curve or the failure criterion curve, a relatively new hybrid strengthening technique that combines the two techniques was proposed by Barros et al. [18] in their experimental program. This hybrid technique is performed by using U-shaped laminates so that the central part of the laminate is applied to the tension surface of the slab adopting NSM approach, while the extremities of the laminate are applied in inclined grooves according to ETS approach. Therefore, this hybrid technique offers a simultaneous improvement for flexural as well as punching shear strength of the slab. The experimental program conducted involved the strengthening of the tested slabs using carbon fiber reinforced polymer (CFRP) U-shaped laminates along with conventional CFRP straight laminates applied according to NSM approach. The laminates were positioned in two different configurations: CONFIG. A and CONFIG. B; with FRP reinforcement ratio of 1% and 2%, respectively. The obtained results from the experimental program showed that the new hybrid strengthening technique offered a good improvement in terms of punching shear strength (about 29.5% improvement for CONFIG. A and 49.5% improvement for CONFIG. B).

Glass fiber reinforced polymer (GFRP) can represent a worthy alternative to CFRP given the economical superiority of the former over the latter. While both GFRP and CFRP are known to be corrosion resistant and to have a long lifespan [19, 20], GFRP has a lower modulus of elasticity, providing higher energy absorption and better damping capacity [21]. Moreover, the glass constituting the main component of glass fibers used for manufacturing GFRP can be recycled and reused making it a more sustainable option than CFRP. Previous studies have been conducted investigating the strengthening of RC flat slabs using GFRP laminates [22-25]. The results showed that the GFRP laminates represented an efficient strengthening method in terms of improving the slab load carrying capacity, flexural strength, stiffness, and shear strength, as well as reducing slab deflections.

The current study aims, using numerical simulation, to investigate the potential of employing the hybrid technique, proposed by Barros et al. [18] to increase the punching strength of RC flat slabs by using glass fiber reinforced polymer (GFRP) laminates. Besides, a parametric study is to be conducted to develop a further understanding of the influence of some important parameters on the slab punching capacity. Furthermore, the analytical approach for determining the punching shear strength using the CSCT developed by Muttoni [4] is employed and the relevant results are to be compared with the results from the numerical simulation to evaluate the efficiency of the CSCT to determine the punching strength of the slabs strengthened with GFRP laminates according to the hybrid technique.

## 2. Numerical simulation

### 2.1 Model description and geometry

Nonlinear finite element (FE) models for the control un-strengthened slab and the CFRP-strengthened slab are developed using Abaqus software (V6.20). The geometry of the slabs and the positioning and dimensions of steel bars and CFRP laminates are adopted from the experimental program [18], and it is shown in Figure 1. Flexural steel reinforcement with a diameter of 10 mm was applied in the tension side of the slab with a reinforcement ratio of 0.53%, whereas a 0.34% reinforcement ratio of 8 mm-diameter steel was applied to the compression side. The CFRP laminates and flexural steel reinforcement were symmetrically applied in both directions. Taking advantage of the double symmetry of the slab, only a quarter slab is modelled, and symmetry supports are introduced to reduce the required computational time of the analysis.

The concrete slab is modeled using 3-D 8-node solid hexahedron-shaped brick elements (C3D8R) with a maximum element size of 10 mm. The element size is chosen according to a mesh sensitivity analysis conducted on the model to eliminate any mesh dependency that can affect the results. The un-strengthened slab model is shown in Figure 2 presenting the slab mesh. The reinforcing steel is modeled using 3-D 2-node truss elements (T3D2), which are only able to carry axial force, with the same element size used for concrete. Regarding the CFRP laminates, they are modeled using the same element type used for concrete (C3D8R) with the same element size.

A perfect bond is assumed between the reinforcing steel bars and concrete by defining the concrete slab as a host element and the steel bars as embedded elements. Similarly, a perfect bond is assumed between the concrete and the CFRP laminates to utilize its full tensile capacity. This assumption is justified based on the observations made by Barros et al. [18] that all the tested slabs failed due to punching shear without any debonding between the laminates and the surrounding concrete, which is attributed to the anchorage benefits provided by the U-shaped laminates. The boundary conditions and loading scenario are modeled to mimic those of the experimental program (see Figure 2 (b)). Three hinges ( $U_2=0$ ) are defined in the model along with the symmetry boundary conditions. A monotonic loading applied on an area of  $100 \times 100 \text{ mm}^2$  is introduced at the center of the slab. The magnitude of the displacement loading is 60 mm, and it is applied on a step time of 10 seconds. A smooth amplitude is specified for the loading step to assure a minimal rate of change of kinetic energy at the beginning and the end of the loading process [26]. For the analysis process, linear shape function is used and reduced integration is specified so that one integration per element is conducted [27].

### 2.2 Material properties and modeling

The main mechanical material properties for concrete, steel, and CFRP are adopted with reference to [18], while the mechanical properties for GFRP are adopted from [28]. Table 1 represents the mechanical properties of all the used materials in this study. Table 1 was directly used to model steel, CFRP, and GFRP.

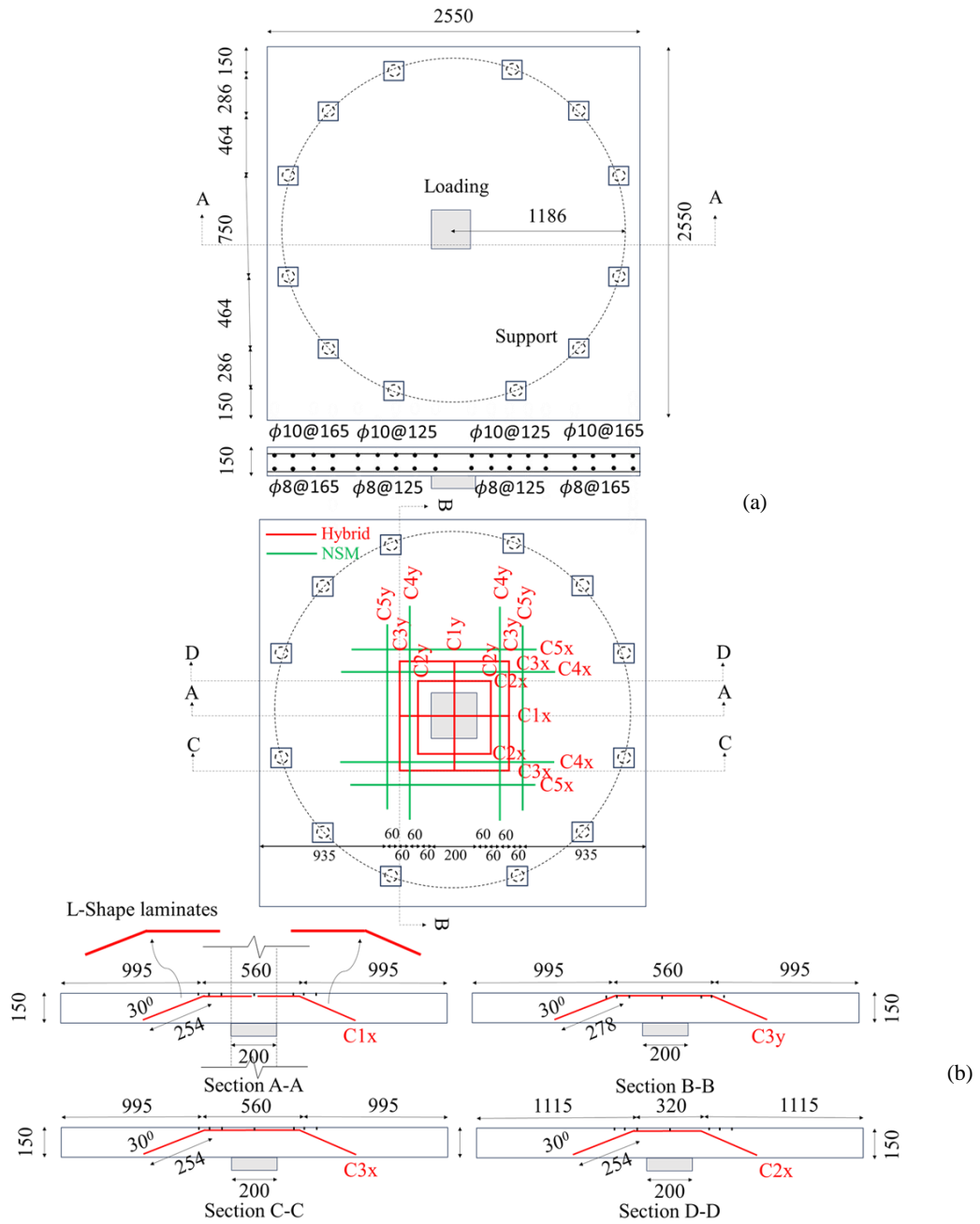


**Figure 1** (a) geometry and boundary conditions of the RC slab, (b) positioning and geometry of the strengthening laminates (dimensions in mm)

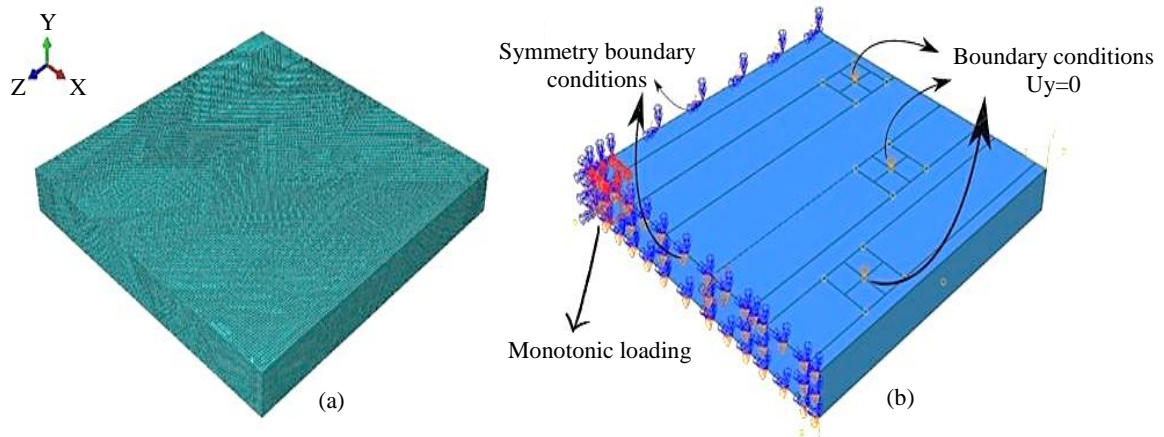


**Figure 2** (a) FE mesh of the RC slab, (b) boundary conditions and loading of the FE model.

Regarding the concrete material modeling, linear and nonlinear behavior are defined in the model. The linear behavior of concrete is defined using the modulus of elasticity value provided in Table 1. For the nonlinear behavior of concrete, it can be defined using one of two models available in Abaqus: concrete smeared cracking model and concrete damage plasticity (CDP) model. The former model assumes that concrete cracking is the most important characteristic of the structure behaviour, and it is intended for applications in which the overall behavior of concrete is dominated by the tensile failure while the compressive failure is not critical according to Abaqus software user manual [27], while the latter model assumes that the main two failure mechanisms are tensile cracking and compressive crushing. The model used to describe the nonlinear behavior of concrete in this study is CDP model. The required plasticity parameters, which convert the uniaxial stress-strain relationship of concrete to biaxial relation, are defined and presented in Table 2. These parameters include the dilation angle ( $\psi$ ),  $\epsilon$  which is the eccentricity of the plastic potential surface, the ratio between the biaxial and the uniaxial compressive yield stresses ( $f_{b0}/f_{c0}$ ),  $K$  which is the ratio of the second stress invariant on the tensile meridian to that on the compressive meridian, and the viscosity parameter ( $\mu$ ).

The nonlinear stress-strain relationship of concrete in compression is governed by Eq. (1) according to Wight and MacGregor [29].

$$\frac{f_c}{f'_c} = \frac{n(\frac{\epsilon_c}{\epsilon_0})}{n-1+(\frac{\epsilon_c}{\epsilon_0})^{nk}} \tag{1}$$

Where  $f_c$  represents the concrete compressive stress,  $f'_c$  represents the compressive strength of concrete based on a cylinder specimen,  $\epsilon_0$  is the strain when the compressive stress reaches  $f'_c$  and its value is governed by Eq. (2),  $n$  is a curve-fitting factor and its value is governed by Eq. (3) (units are in psi), and  $K$  is a controlling factor for the slopes of the rising and falling branches of the stress-strain curve and its value is governed by Eq. (4).

$$\epsilon_0 = \frac{f'_c}{E_c} \left(\frac{n}{n-1}\right) \tag{2}$$

Where  $E_c$  represents the initial tangent modulus, and its value is taken as  $57,000 \sqrt{f'_c}$  for normal weight concrete.

$$n = 0.8 + \left(\frac{f'_c}{2500}\right) \tag{3}$$

$$K = \begin{cases} 1 & \text{for } \frac{\epsilon_c}{\epsilon_0} \leq 1 \\ 0.67 + \left(\frac{f'_c}{9000}\right) & \text{for } \frac{\epsilon_c}{\epsilon_0} > 1 \end{cases} \tag{4}$$

**Table 1** Material mechanical properties.

Material	Mechanical properties						
	$f'_c$ (Mpa)	$E_c$ (Gpa)	$f_{sy}$ (Mpa)	$f_{su}$ (Mpa)	$E_l$	$f_{lu}$	$\epsilon_u$ (%)
Concrete	43	31.8	–	–	–	–	–
Steel ( $\phi 8$ )	–	–	545.9	680.1	–	–	–
Steel ( $\phi 10$ )	–	–	530.6	646.4	–	–	–
CFRP	–	–	–	–	165.5	2896.5	17.5
GFRP	–	–	–	–	48	1200	25

$f_{sy}$  and  $f_{su}$ : yield and ultimate tensile strength of steel,  $E_l$ ,  $f_{lu}$ , and  $\epsilon_u$ : modulus of elasticity, tensile strength, and ultimate tensile strain of FRP.

**Table 2** CDP model input parameters.

$\psi$	$\epsilon$	$f_{b0}/f_{c0}$	$K$	$\mu$
35°	0.1 m	1.16	0.67	0

A modified tension stiffening model developed by Wahalathantri et al. [30] (see Figure 3) was used to define the concrete post-failure tensile behavior.

Furthermore, the concrete damage in compression and tension is described in the model by defining compression and tension damage parameters ( $d_c$  and  $d_t$ ) which were determined using Equations (5) and (6). These parameters are functions of the plastic strains in both compression and tension ( $\epsilon_c^{-pl}$  and  $\epsilon_t^{-pl}$ ). Calculation of the plastic strains were performed using inelastic strains in compression and tension ( $\epsilon_c^{-in}$  and  $\epsilon_t^{-in}$ ) by Eqs. (7) and (8).

$$d_c = 1 - \frac{f_c}{f'_c} \tag{5}$$

$$d_t = 1 - \frac{\sigma_t}{\sigma_{t0}} \tag{6}$$

$$\varepsilon_c \sim pl = \varepsilon_c \sim in - \frac{d_c}{(1-d_c)} \frac{f_c}{E_{0c}} \tag{7}$$

$$\varepsilon_t \sim pl = \varepsilon_t \sim in - \frac{d_c}{(1-d_t)} \frac{\sigma_t}{E_{0t}} \tag{8}$$

Where  $\sigma_t$  is the concrete tensile stress.  $E_{0c}$  is the modulus of elasticity of concrete in the uniaxial compression, while  $E_{0t}$  is young's modulus of concrete in uniaxial tension.

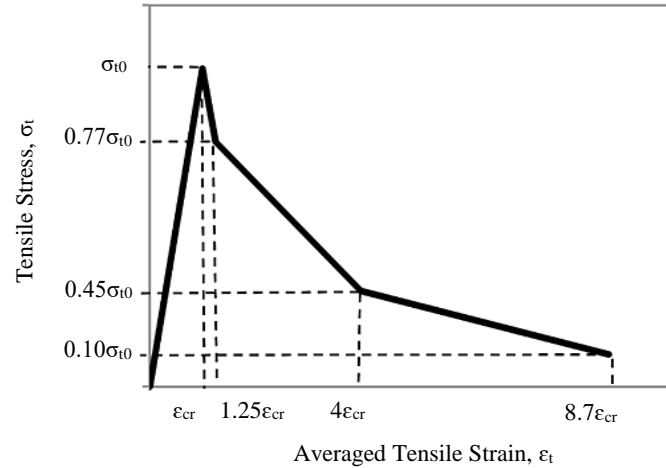


Figure 3 Modified tension stiffening model [30].

2.3. Validation of the FE model

The results from the un-strengthened FE model and the CFRP-strengthened FE model are validated against their corresponding results from the experimental program conducted by Barros et al. [18]. The load versus central deflection curve is used in the validation process. Figure 4 shows a comparison between the load-deflection from the experimental and FE models for the un-strengthened and CFRP-strengthened slabs. As shown in the figure, a good agreement is reached between the FE results and the experimental results for both the un-strengthened and the CFRP-strengthened slab. For the un-strengthened slab, the FE model understates the value of the maximum load carrying capacity of the slab by about 8%, while the performance of the CFRP-strengthened FE model was more accurate in terms of predicting the maximum load carrying capacity and its corresponding central deflection value with a true error value of about 0.7%.

So, after the FE models proved their capability to reflect the real behavior of the RC strengthened and un-strengthened slabs, they can confidently be used to investigate the effect of changing the strengthening material on the slab punching strength. Also, the FE models can confidently be used to conduct a parametric study on the RC slab to develop a deeper understanding of the effect of some key parameters on the slab punching capacity.

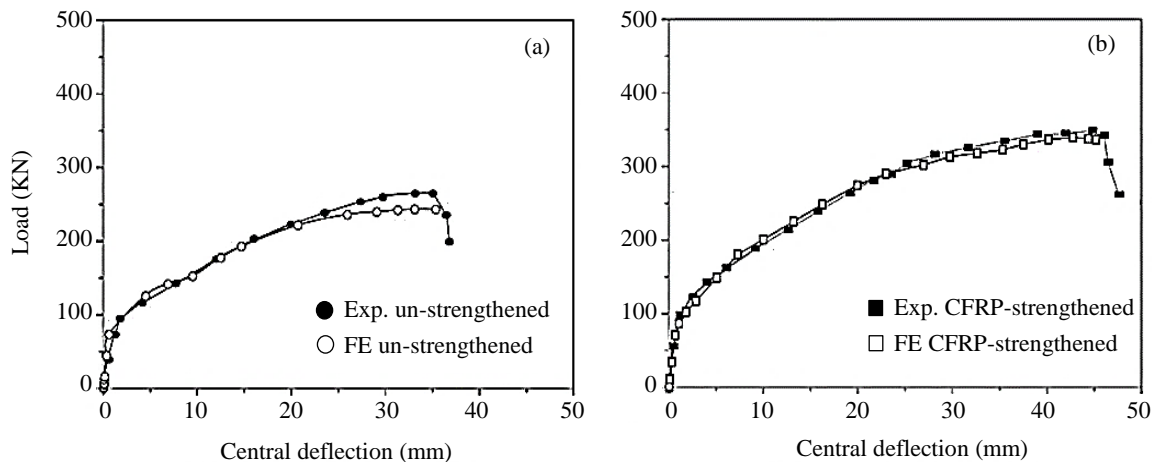
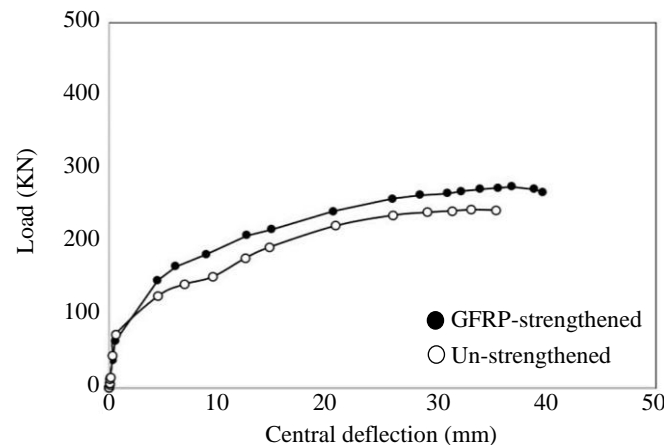


Figure 4 (a) load-deflection curve of the FE un-strengthened slab model against the experiential un-strengthened slab, (b) load deflection curve of the FE CFRP-strengthened slab model against the experiential CFRP-strengthened slab.

### 3. Results

#### 3.1. GFRP strengthening

Based on the observations in the experimental program that all the tested slabs failed due to punching shear, the ultimate load carrying capacity of the slabs can then be considered to directly represent the punching shear strength of the slabs. The load versus central deflection curve for the GFRP-strengthened slab along with the un-strengthened slab is presented in Figure 5. As shown in the figure, strengthening the slab with GFRP laminates according to the hybrid technique resulted in improving the slab's punching shear strength by about 13% with reference to the un-strengthened slab. For comparison, using CFRP laminates in the same configuration resulted in increasing the punching strength of the slab by about 39%. The higher percentage of improvement provided by CFRP laminates over GFRP laminates is due to the higher modulus of elasticity as well as the tensile strength of CFRP compared to GFRP. However, the improvement in the slab's punching strength provided by using GFRP laminates is reasonable considering its economic advantage over CFRP. The values of the punching shear strength and its corresponding central deflection for the un-strengthened, CFRP-strengthened, and GFRP-strengthened slab are presented in Table 3.



**Figure 5** Comparison between the load-deflection curve of the un-strengthened and GFRP-strengthened slab.

**Table 3** Ultimate load carrying capacity and its corresponding central deflection for all FE slab models.

	$P_u$ (KN)	$\Delta_u$ (MM)
Un-strengthened	244.1	35.2
GFRP-strengthened	275.7	38.8
CFRP-strengthened	339.3	42.9

$P_u$ : ultimate load carrying capacity,  $\Delta_u$ : central deflection corresponding to the ultimate load.

### 4. Parametric study

This section aims to build a better grasp of the influence of some key parameters on the punching capacity of the GFRP-strengthened slab. The investigated parameters are the cross-sectional area of the strengthening laminates, the geometry of the U-shaped strengthening laminates, and the compressive strength of concrete.

Figure 6 (a) shows the influence of changing the cross-sectional area of the laminates on the RC slab's load versus central deflection relationship. The original cross-sectional area of the strengthening laminates is  $1.4 \times 10 \text{ mm}^2$  and it's denoted as CSA\_0, while another two cross-sectional areas used are  $1.4 \times 15 \text{ mm}^2$  and  $1.4 \times 20 \text{ mm}^2$  and they are denoted as CSA\_1 and CSA\_2, respectively (see Figure 6 (b)). The results showed that (see Figure 6 (a)) increasing the cross-sectional area of the GFRP laminates from that used in CSA\_0 to that applied in CSA\_1 caused the punching shear strength of the slab to increase by about 3.7%, while further increasing the cross-sectional area to that applied in CSA\_2 caused the punching shear strength of the slab to increase by about 7% compared to CSA\_0. Therefore, the punching shear strength of the slab increases by increasing the cross-sectional area of the strengthening laminates.

Another parameter to be investigated is the geometry of the U-shaped laminates, specifically, the horizontal angle by which the extremities of the laminates are introduced. The original horizontal angle of the laminate extremities is  $30^\circ$  and it's denoted as HA\_0, while the horizontal to be investigated is  $45^\circ$  and it's denoted as HA\_1 (see Figure 6 (d)). The value of the horizontal angle was adopted aiming for the cross-sectional area of the laminates to be perpendicular to the punching shear cracks that take place on an angle of  $45^\circ$  [31, 32]. Figure 6 (c) shows a comparison between the load-deflection curve for the RC slab strengthened with HA\_1 laminates and the RC slab strengthened with the original laminates. As shown in the figure, changing the horizontal angle of the U-shaped laminates extremities from HA\_0 to HA\_1 resulted in a slight improvement of about 1% in the punching shear strength of the slab.

The last parameter to be investigated is the compressive strength of concrete ( $f'_c$ ). The original  $f'_c$  value is 43 MPA, while additional two values of 38 MPA and 33 MPA are adopted. The goal of studying this parameter is to assess the influence of changing  $f'_c$  on the contribution of strengthening in improving the punching capacity of the slab. Table 4 presents the punching strength of RC slabs with different  $f'_c$  values, along with the percentage of improvement of punching shear strength provided due to strengthening for every  $f'_c$  value. The results evidenced that the contribution of strengthening becomes more significant in terms of improving the punching capacity of the slab as the value of  $f'_c$  decreases. This behavior can be linked to the higher susceptibility for weaker RC slabs to fail due to punching shear; thus, strengthening becomes more effectual.

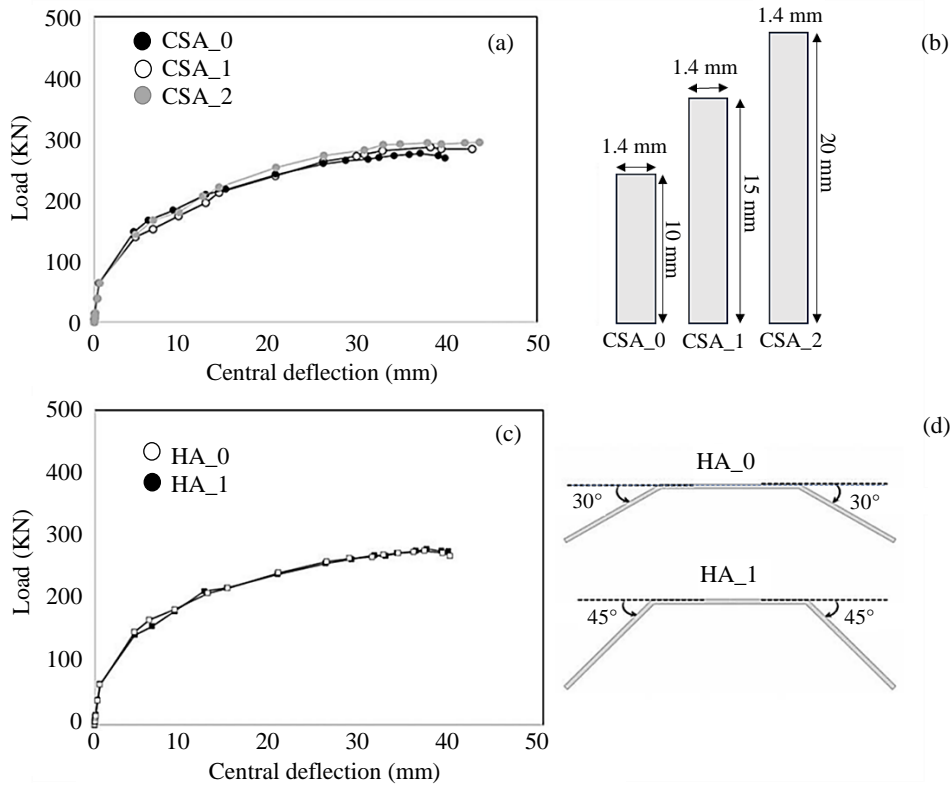


**Figure 6** (a) effect of changing the cross-sectional area of the strengthening laminates on the load-deflection curve, (b) different laminates’ cross-sectional areas, (c) effect of changing the geometry of the strengthening laminates on the load-deflection curve, (d) geometry of the U-shaped laminates.

**Table 4** effect of changing compressive strength of concrete on the RC slab punching shear strength.

	$P_u$ (KN)	Increase in $P_u$ (%)
Un-strengthened ( $f'_c = 43$ MPA)	244.1	
GFRP-strengthened ( $f'_c = 43$ MPA)	275.6	13%
Un-strengthened ( $f'_c = 38$ MPA)	229.5	
GFRP-strengthened ( $f'_c = 38$ MPA)	262.6	14.4%
Un-strengthened ( $f'_c = 33$ MPA)	199.1	
GFRP-strengthened ( $f'_c = 33$ MPA)	231.2	16.1%

**5. Analytical prediction of punching shear strength**

This section aims to evaluate the efficiency of applying the simplified CSCT to analytically predict the punching shear strength of the un-strengthened slab as well as the GFRP-strengthened slab adopting the hybrid technique. The compressive strength of the slabs investigated in this section was 43 MPa, the laminates in the strengthened slab had a cross-sectional area of  $1.4 \times 10 \text{ mm}^2$  with angle of inclination at the extremities of  $30^\circ$ . According to the CSCT, the punching shear strength is represented by the intersection point between the load-rotation curve and the failure criterion (see Figure 7). For the load-rotation curve, it can either be obtained using numerical simulation or by calculating the slab rotation ( $\psi$ ) using the simplified expression presented in Eq. 9. This expression is a modified version developed by Barros et al. [18] to account for the concepts of equivalent tensile strength ( $f_{s,eq}$ , Eq. (10)) and elasticity modulus ( $E_{s,eq}$ , Eq. (11)) of flexural steel and equivalent effective depth ( $d_v$ , Eq. (12)) of the slab.

$$\psi = 1.5 \frac{r_s}{d_v} \frac{f_{s,eq}}{E_{s,eq}} \left( \frac{V}{V_{flex}} \right)^{\frac{3}{2}} \tag{9}$$

Where  $r_s$  represents the radius of isolated circular slab element;  $V$  and  $V_{flex}$  represent the shear force which is applied on the slab and the shear force associated with the slab’s flexural capacity, respectively.

$$f_{s,eq} = \frac{A_s \cdot f_{sy} + A_f \frac{E_f}{E_s} f_{fe}}{A_s + A_f \frac{E_f}{E_s}} \tag{10}$$

Where  $A_s$ ,  $f_{sy}$ , and  $E_s$  are the cross-sectional area, yield strength, and modulus of elasticity of flexural steel, respectively, and  $A_f$  and  $f_{fe}$  are the cross-sectional area and effective tensile strength of the strengthening laminates, respectively. Where  $d_s$  is the effective depth of flexure steel and  $d_f$  is the internal arm of the strengthening laminates.

$$E_{s,eq} = \frac{A_s \cdot E_s + A_f \frac{E_f}{E_s} \cdot E_f}{A_s + A_f \frac{E_f}{E_s}} \tag{11}$$

Where  $E_s$  and  $E_f$  are the moduli of elasticity of flexure steel and strengthening laminates, respectively.

$$d_v = \frac{A_s \cdot d_s + A_f \frac{E_f}{E_s} \cdot d_f}{A_s + A_f \frac{E_f}{E_s}} \tag{12}$$

For the failure criterion, it can be obtained using the expression presented in Eq. (13). This expression is a semi-empirical formulation that relates the punching shear strength ( $V_r$ ) of the slab to the crack width which is, in turn, assumed to be the product of the slab equivalent depth and the slab rotation ( $d_v \cdot \psi$ ) [33] based on the results from previous studies [5-6].

$$\frac{V_r}{b_o \cdot d_v \cdot \sqrt{f'_c}} = \frac{3/4}{1 + 15 \cdot \frac{\psi \cdot d_v}{d_{go} + d_g}} \tag{13}$$

Where  $b_o$  is the critical perimeter of the punching shear failure and it's taken as  $d_v/2$ ,  $d_{go}$  represents the reference size of the aggregate and its value is taken as 16 mm, and  $d_g$  represents the maximum size of the aggregate.

Figure 7 presents the analytical prediction of the CSCT to the punching shear strength of the un-strengthened as well as the GFRP-strengthened slab. As shown in this figure, the CSCT was able to predict the punching shear strength for both slabs with good accuracy. The ratio between the numerical and analytical punching shear strength of the un-strengthened and the GFRP-strengthened slab is 0.97 and 1.02, respectively.

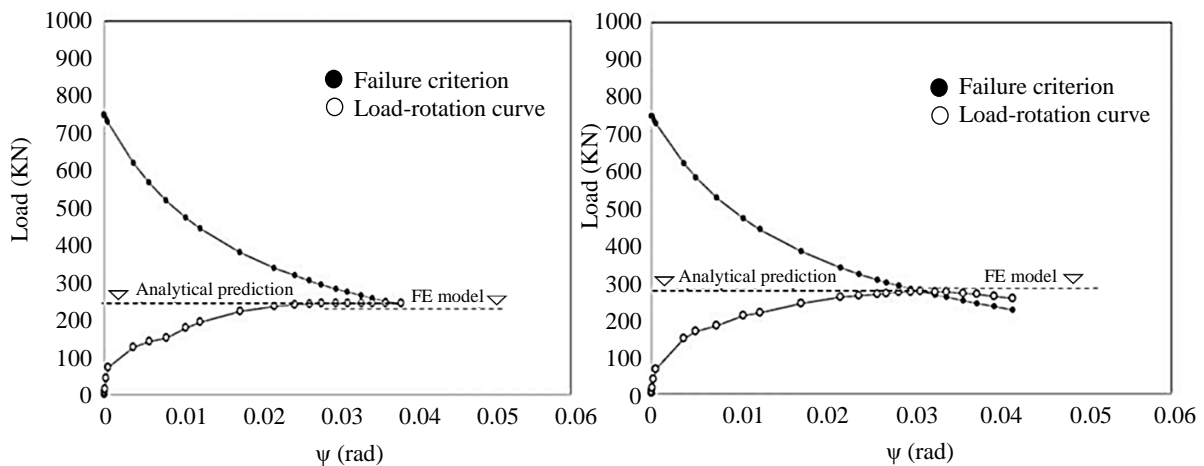


**Figure 7** Analytical prediction of the punching shear strength; (a) un-strengthened slab, (b) GFRP-strengthened slab.

**6. Conclusions**

The current study has numerically investigated the potential of using GFRP laminates to strengthen existing RC flat slabs by adopting a hybrid strengthening technique. Also, a parametric study was conducted to assess the influence of some key parameters on the punching shear strength of the slab. Moreover, the efficiency of the analytical approach to calculate the punching shear strength using the critical shear crack theory was evaluated for RC flat slabs strengthened with GFRP laminates according to the hybrid technique. Based on the obtained results, the following can be concluded:

- Strengthening RC flat slabs with GFRP laminates according to the hybrid technique resulted in a reasonable improvement in terms of punching shear strength (about 13% improvement compared to the un-strengthened slab).
- Increasing the cross-sectional area of the GFRP strengthening laminates caused the punching shear strength of the slab to increase by about 3.7% for 50% increase in the cross-sectional area; and about 7% for 100% increase in the cross-sectional area.
- Changing the horizontal angle by which the extremities of the U-shaped GFRP laminates are introduced to be approximately perpendicular to the direction of punching shear cracks resulted in an insignificant improvement in terms of the slab punching shear strength (about 1% improvement).
- The contribution provided by the strengthening of RC flat slabs against punching shear failure becomes more significant for slabs with lower concrete compressive strength.
- The critical shear crack theory represented an accurate prediction for the punching shear strength of the un-strengthened slab as well as the slab strengthened with GFRP laminates adopting the hybrid technique (the ratio between the numerical and analytical punching shear strength is 0.97 for the un-strengthened slab, and 1.02 for the GFRP-strengthened slab).

**7. References**

[1] Russel J. Progressive collapse of reinforced concrete flat slab structures [dissertation]. Nottingham: University of Nottingham; 2015.

- [2] Sissakis K, Sheikh SA. Strengthening concrete slabs for punching shear with carbon fibre reinforced polymer laminates. *ACI Struct J*. 2007;104(5):49-59.
- [3] Bartolac M, Damjonovic D, Dvnjak I. Punching strength of flat slabs with and without shear reinforcement. *Gradevinar*. 2015; 67(8):771-86.
- [4] Muttoni A. Punching shear strength of reinforced concrete slabs without transverse reinforcement. *ACI Struct J*. 2008;105(4): 440-50.
- [5] Walraven JC. Fundamental analysis of aggregate interlock. *J Struct Div*. 1981;107(11):2245-70.
- [6] Vecchio FJ, Collins MP. The modified compression-field theory for reinforced concrete elements subjected to shear. *ACI Struct J*. 1986;83(2):219-31.
- [7] Lapi M, Ramos AP, Orlando M. Flat slab strengthening techniques against punching-shear. *Eng Struct*. 2019;180:160-80.
- [8] Hassanzadeh G, Farhang A. Strengthening of bridge slabs with respect to punching—in Swedish (Forstärkning av brobanepaltor med hänsyn till stansning) [thesis]. Stockholm: Institute of Technology; 1995. [In Swedish]
- [9] Ramos A, Lúcio V, Regan P. Repair and strengthening methods of flat slabs for punching. *International Workshop on Punching Shear Capacity of RC Flat Slabs*; 2000; Stockholm, Sweden. p. 125-34.
- [10] Hassanzadeh G, Sundqvist H. Strengthening of bridge slabs on columns. *Nord Concr Res*. 1998;21:23-34.
- [11] Jansze W. Strengthening of reinforced concrete members in bending by externally bonded steel plates [dissertation]. Delft: Delft University; 1997.
- [12] El-Hacha R, Rizkalla SH. Near-surface-mounted fiber-reinforced polymer reinforcements for flexural strengthening of concrete structures. *ACI Struct J*. 2004;101(5):717-26.
- [13] Moreno C, Ferreira D, Bennani A, Sarmento A, Noverraz M. Punching shear strengthening of flat slabs: CFRP and shear reinforcement. *Concrete – Innovation and Design, fib Symposium*; 2015 May 18-20; Copenhagen, Denmark. p. 1-16.
- [14] Rezazadeh M. Innovative methodologies for the enhancement of the flexural strengthening performance of NSM CFRP technique for RC beams [dissertation]. Braga: University of Minho; 2015.
- [15] Rezazadeh M, Costa I, Barros J. Influence of prestress level on NSM CFRP laminates for the flexural strengthening of RC beams. *Compos Struct*. 2014;116:489-500.
- [16] Rezazadeh M, Cholostiakow S, Kotynia R, Barros J. Exploring new NSM reinforcements for the flexural strengthening of RC beams: experimental and numerical research. *Compos Struct*. 2016;141:132-45.
- [17] Meisami MH, Mostofinejad D, Nakamura H. Punching shear strengthening of two-way flat slabs using CFRP rods. *Compos Struct*. 2013;99:112-22.
- [18] Barros J, Rezazadeh M, Laranjeira J, Hosseini M, Mastali M, Ramezansafat H. Simultaneous flexural and punching strengthening of RC slabs according to a new hybrid technique using U-shape CFRP laminates. *Compos Struct*. 2017;159:600-14.
- [19] Feng P, Wang J, Wang Y, Loughery D, Niu D. Effects of corrosive environments on properties of pultruded GFRP plates. *Compos B Eng*. 2014;67:427-33.
- [20] Ibrahim A, Salem S, Khalil A, El-Kateb M. Experimental investigation for moment redistribution in continuous RC beams top strengthened with CFRP and steel plates. *IOP Conf Ser: Mater Sci Eng*. 2020;809(1):012007.
- [21] Hawileh RA, Abu-Obeidah A, Abdalla JA, Al-Tamimi A. Temperature effect on the mechanical properties of carbon, glass and carbon–glass FRP laminates. *Constr Build Mater*. 2015;75:342-8.
- [22] Chen CC, Li CY. Punching shear strength of reinforced concrete slabs strengthened with glass fiber-reinforced polymer laminates. *ACI Struct J*. 2005;102(4):535-42.
- [23] El-Salakawy E, Soudki K, Polak MA. Punching shear behavior of flat slabs strengthened with fiber reinforced polymer laminates. *J Compos Constr*. 2004;8(5):384-92.
- [24] Mohamed OA, Kewalramani M, Khattab R. Fiber reinforced polymer laminates for strengthening of RC slabs against punching shear: a review. *Polymers*. 2020;12(3):685.
- [25] Abdulrahman BQ, Aziz OQ. Strengthening RC flat slab-column connections with FRP composites: a review and comparative study. *J King Saud Univ Eng Sci*. 2021;33(7):471-81.
- [26] Salem S, Ibrahim A, El-Kateb M, Khalil A, Fouda MA. Effect of NSM technique on moment redistribution in top strengthened RC continuous beams. *Jordan J Civ Eng*. 2022;16(3):457-71.
- [27] Smith M. Abaqus user's manual. Rhode Island: Dassault Systèmes Simulia Corp; 2009.
- [28] Peters St. Handbook of Composites. 2<sup>nd</sup> ed. London: Chapman and Hall; 1998.
- [29] Wight JK, MacGregor JG. Reinforced concrete mechanics and design. 6<sup>th</sup> ed. New Jersey: Prentice Hall; 2012.
- [30] Wahalathantri BL, Thambiratnam DP, Chan THT, Fawzia S. A material model for flexural crack simulation in reinforced concrete elements using ABAQUS. *Proceedings of the First International Conference on Engineering, Designing and Developing the Built Environment for Sustainable Wellbeing*; 2011; Brisbane, Australia. p. 260-4.
- [31] Abdel-Rahman AM, Hassan NZ, Soliman AM. Punching shear behaviour of reinforced concrete slabs using steel fibres in the mix. *HBRC J*. 2018;14(3):272-81.
- [32] Jose P, Pasha J. Punching shear in concrete flat slabs supported on slender edge steel columns [thesis]. Stockholm: KTH Royale Institute of Technology; 2020.
- [33] Muttoni A. Shear and punching strength of slabs without shear reinforcement (Schubfestigkeit und Durchstanzen von Platten ohne Querkarfbewehrung). *Beton-und Stahlbetonbau*. 2003;98(2):74-84. [In German]